Oxygen Exchange and Diffusion in Uranium Dioxide Single Crystals

SA Joyce[*], JA Stultz[†], MT Paffett[*]

[*]Los Alamos National Laboratory, Los Alamos NM 87544 USA
[†]US Borax, Boron, CA

There are a number of solid uranium oxides ranging from U(II)O to U(VI)O_3, with essentially a continuous range of stoichiometries from UO_{2-x} up to UO_3. UO_2 is fairly stable under normal ambient conditions and is the form often used in oxide fuels and in many waste forms. There are concerns related to changes in the chemical and mechanical properties of the UO_2 upon bulk oxidation. Bulk oxidation proceeds by at least two steps: 1) oxygen incorporation into surface and 2) subsequent diffusion into the bulk. We have examined both steps using water adsorption on single crystal UO_2. In the first set of experiments, a $U^{16}O_2$ sample is exposed ^{18}O-labeled water and investigated using electron stimulated desorption (ESD). In ESD, electron irradiation leads to the desorption of oxygen ions from the surface layer only. For clean UO_2 surfaces, only $^{16}O^+$ is observed; both ^{18}O and ^{16}O are seen for water-exposed surfaces, even at cryogenic temperatures. The exchanged ^{18}O, however, remains at the surface up to temperatures as high as 650K, above which it decreases due to diffusion into the bulk. In the second set of experiments, a UO2 surface is made oxygen deficient by ion sputtering. This reduced surface is reactive to water leading to H_2 desorption at 400K. By annealing the sample to various temperatures prior water exposure, we find the surface reoxidizes by diffusion of oxygen out of the bulk at ~700K. From these studies, we can determine the diffusion constant of oxygen in UO_2 at 700K. The calculated D (~10^{-17} cm^2/sec) is in good agreement with extrapolations from previous high temperature (>1200K) studies.

Acknowledgements: This work was supported by Los Alamos National Laboratory LDRD. JS acknowledges the Seaborg Institute for postdoctoral support.

Molecular Magnetism in Some Neptunyl (+1, +2) Complexes

A. Nakamura[*], M. Nakada[*], T. Nakamoto[*], T. Kitazawa[†] and M. Takeda[†]

[*]Advanced Science Research Center, Japan Atomic Energy Agency, Tokai, Ibaraki 319-1195, Japan

[†] Department of Chemistry, Faculty of Science, Toho University, Funabashi, Chiba 274-8510, Japan

The magnetic-property study of actinide (5f) complexes is few, compared with its intermetallic systems where the so-called heavy-fermion type exotic physical (electronic and magnetic) properties have been intensively studied. However, to elucidate the magnetic property of actinide complexes is of particular interest from the viewpoint of 5f low-dimensional (low-D) molecular magnetism. We are interested in the magnetic property of neptunyl (+1,+2) (Np(V,VI): $5f^{2,1}$) complexes in which strongly-bonded linear neptunyl $(O=Np=O)^{+1,+2}$ monocations form unique 0, 1 to 3D network structures extended by the so-called 'cation-cation bond (CCB)'. Lately, transition-metal (3d) and lanthanide (4f) clusters, rings and complexes have been receiving increasing attention as a nanoscale and/or molecular magnet.[1] Also in this context, actinide complexes where the 5f electrons are known to exhibit a marginal character between the 3d and 4f electrons are expected to represent a novel class of nanomagnetic materials.

Though only a few of them are investigated up to now, magnetic-susceptibility and ^{237}Np Mössbauer study of our group[2] has revealed that oxygen-coordinated neptunyl (+1) (Np(V)) complexes exhibit intriguing common feature as a neptunyl-molecular magnet and yet diversed magnetic character depending on the specific neptunyl network structure from a Curie-Weiss paramagnet to ferro- and meta-magnets.

We are lately extending such study to neptunyl (+2) (Np(VI)) complexes; a trinitrato complex, $NH_4[NpO_2(NO_3)_2]$(**1**), and two (acetyl-aceton (acac=$C_5H_7O_2^-$) or trinitrato) pyridine (py=C_5H_5N) complexes, $NpO_2(acac)_2py$(**2**) and $NpO_2(NO_3)_2byp$(**3**) (where bpy(bipridine) =$C_{10}H_8N_2$).[3] In the latter two (**2**, **3**) systems, one or two of the coordinating non-nyl oxygens are substituted with nitrogen(s). Plausibly related to this O→N substitution in the Np coordination environment, **2** and **3** are found to exhibit many striking magnetic features (peculiar field-dependent paramagnetic behavior up to room temperature, very large magnetic relaxation effect at low temperature, etc.) different from those of **1** and other known neptunyl (+1, +2) systems. These results are discussed in connection with their microscopic ^{237}Np Mössbauer data.

1. O. Kahn, 'Molecular Magnetism', Wiley-VCH (N.Y), 1993.
2. T. Nakamoto, M. Nakada and A. Nakamura, J. Nucl. Sci. Technology, Suppl.**3**, 102 (2002).
3. A. Nakamura, M. Nakada, T. Nakamoto, T. Kitazawa and M. Takeda, submitted to J. Phys. Soc. Jpn. Suppl. (2006) (Proc. ASRC-WYP-Symp.(2005)).

Nanostructured Actinide Compounds

S.V. Krivovichev[*], P.C. Burns[†], I.G. Tananaev[‡], B.F. Myasoedov[‡]

[*]St. Petersburg State University, St.Petersburg 199034 Russia
[†]University of Notre Dame, Notre Dame IN 46556 USA
[‡]Institute of Physical Chemistry, Russian Academy of Sciences, Moscow 119991 Russia

INTRODUCTION

Nanostructure is the term generaly used to describe the structure with at least one dimension in the nanometer range (1-1000 nm). These include nanocrystals and clusters (quantum dots), nanowires, nanotubes, thin films and superlattices (3-D structures). Usually, nanostructures have more reactive surfaces and exhibit new functions for the same chemical composition in comparison with the bulk material. Investigations of organization of matter at the nano-level are under way in many chemical systems with present and potential applications in nanotechnology. Recently, nanoscale structures were reported for the first time for actinide-containing compounds as well [1] and here we briefly summarize our recent results in the field.

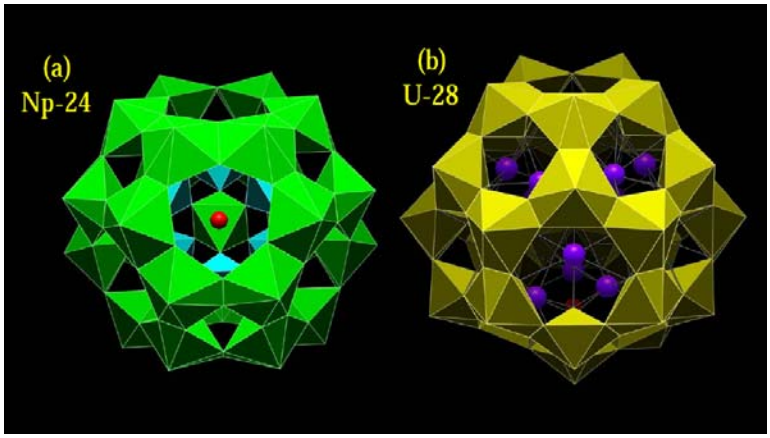

Fig. 1. Np-24 and U-28 nanospheres [2].

NANOCLUSTERS: 0D NANOSTRUCTURES

Burns et al. [2] reported the synthesis and characterization of a new family of self-assembling, f-ion (An) nanospheres with compositions such as $K_{16}(H_2O)_2(UO_2)(O_2)_2(H_2O)_2[(UO_2)(O_2)_{1.5}]_{28}^{14-}$ and $Li_6(H_2O)_8NpO_2(H_2O)_4[(NpO_2)(O_2)(OH)]_{24}^{20-}$ that are comprised of linear actinyl-peroxide building blocks. Their molecular units are composed of 24, 28 or 32 uranyl peroxide polyhedra (designated U-24, U-28 and U-32), or 24 neptunyl peroxide polyhedra (designated Np-24). The nanospheres have diameters of approximately 16.4, 17.7, and 18.6 Å (between the centers of bounding O atoms). The nanospheres are comprised of two types of actinyl peroxide polyhedra. U-24, U-32 and Np-24 contain topologically identical $(AnO_2)(O_2)_2(OH)_2$ hexagonal bipyramids, with O atoms of the actinyl ions constituting apices of the bipyramids, and peroxide groups form two of the equatorial edges of the polyhedra.

1D NANOSTRUCTURES: URANYL-BASED NANOTUBULES

Krivovichev et al. [3,4] reported synthesis and structures of two uranium(VI) compounds, $K_5[(UO_2)_3(SeO_4)_5](NO_3)(H_2O)_{3.5}$ (**1**) and $(C_4H_{12}N)_{14}[(UO_2)_{10}(SeO_4)_{17}(H_2O)]$ (**2**), containing nanometer-sized tubules formed by corner sharing of $U^{6+}O_7$ pentagonal bipyramids and SeO_4 tetrahedra. The most intriguing feature of the structures of compounds **1** and **2** is in that they contain isolated nanotubules formed by corner sharing of $U^{6+}O_7$ pentagonal bipyramids and SeO_4 tetrahedra (Fig. 2). Such nanometer-scale tubules formed by two types of coordination polyhedra are new for inorganic oxosalts. The uranyl selenate nanotubules in the structures of **1** and **2** have circular cross-sections with outer diameters of 17 and ~ 25 Å (= 1.7 and 2.5 nm), respectively. The crystallographic free diameters of the tubules are 4.7 and 12.7 Å for **1** and **2**, respectively.

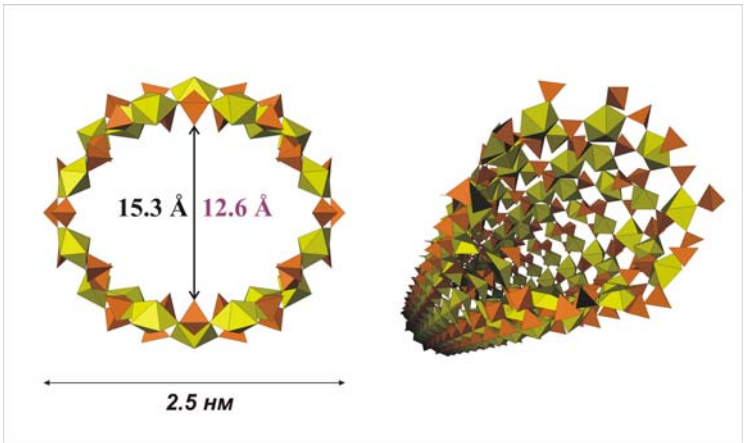

Fig. 2. Uranyl selenate nanotubules in the structure of **2**.

2D NANOSTRUCTURES: NANOCOMPOSITES

Hybrid organic-inorganic highly ordered nanocomposites have been recently reported by Krivovichev et al. [5,6]. In these structures, interfacial interactions between organic and inorganic substructures can be studied by charge-density matching principle. Application of this principle to actinide compounds requires special attention since surface area of actinide-based 2D units is higher than that of other inorganic oxysalts units (i.e. metal phosphates). The charge-density matching principle is, however, observed either through tail interdigitation (for long-chain monoamines) or incorporation of acid-water interlayers into organic substructure (for long-chain diamines). In some compounds, protonated amine molecules form cylindrical micelles that involves self-assembly governed by competing hydrophobic/hydrophillic interactions [5]. The flexible inorganic complexes present in the reaction mixture could then form around cylindrical micelles to produce highly undulated 2D sheets or nanotubules.

Thanks are due to the Ministry of Science and Education of the Russian Federation and RFBR for financial support.

1 Th. Albrecht-Schmitt, Angew. Chem. Int. Ed. **44**, 4836 (2005).
2 P.C. Burns, K.-A. Hughes Kubatko, G. Sigmon, B.J. Fryer, J.E. Gagnon, M.R. Antonio, L. Soderholm, Angew. Chem. Int. Ed. **44**, 2135 (2005).
3 S.V. Krivovichev, V. Kahlenberg, R. Kaindl, E. Mersdorf, I.G. Tananaev, B.F. Myasoedov, Angew. Chem. Int. Ed. **44**, 1134 (2005).
4 S.V. Krivovichev, V. Kahlenberg, R. Kaindl, E. Mersdorf, I.G. Tananaev, B.F. Myasoedov, J. Amer. Chem. Soc. **127**, 1072 (2005).
5 S.V. Krivovichev, V. Kahlenberg, R. Kaindl, E. Mersdorf, Eur. J. Inorg. Chem. **2005**, 1653 (2005).
6 S.V. Krivovichev, I.G. Tananaev and B.F. Myasoedov, MRS Proceedings. *In press* (2006).

Hydrous PuO_{2+x}(s): Solubility and Thermodynamic Data

V. Neck*, M. Altmaier*, C.M. Marquardt*, A. Seibert†, J.I. Yun*, Th. Fanghänel*

*Institut für Nukleare Entsorgung, Forschungszentrum Karlsruhe, D-76021 Karlsruhe, Germany
†European Commission, JRC, Inst. for Transuranium Elements, D-76125 Karlsruhe, Germany

SOLUBILITY AND REDOX POTENTIALS

The solubility and redox reactions of Pu(IV) hydrous oxide were analyzed by comparing total Pu concentrations, oxidation state distributions and simultaneously measured redox potentials under air (Rai et al.[1]) and under Ar containing only traces of O_2 (present work). Combing all information strongly indicates that O_2 is scavenged by solid PuO_2(s,hyd) yielding mixed valent PuO_{2+x}(s,hyd) = $(Pu^V)_{2x}(Pu^{IV})_{1-2x}O_{2+x}$(s,hyd) according to the net reaction of the water-catalyzed oxidation mechanism proposed by Haschke et al.[2]:

$$PuO_2(s,hyd) + x/2\ O_2(g) \rightarrow PuO_{2+x}(s,hyd)$$

At pH < 3 (region A in Fig.1), the oxidized fractions of PuO_{2+x}(s,hyd) (ca. 10 % in the studies of Rai et al.[1] under air and 0.5 % in the present experiment) are completely soluble and lead to a constant level of [Pu(V)] + [Pu(VI)] (under air), which is correlated and limited to the amount of oxygen in the system and/or the amount of oxidized Pu in the original Pu(IV) stock solution. In the present study under Ar, the samples at pH < 2.5 did not contain Pu(VI) but predominantly Pu(V) and Pu(III). At pH > 3, the aqueous Pu concentration is dominated by Pu(V) for both the studies under air or Ar. The maximum concentration of PuO_2^+, decreasing with slope -1 in a logarithmic plot vs. pH (regions B and C in Fig.1), is limited to the solubility of PuO_{2+x}(s,hyd) considered as solid solution $(PuO_{2.5})_{2x}(PuO_2)_{1-2x}$(s,hyd). Defining the solubility product as

$$K_{sp}(PuO_{2.5} \text{ in } PuO_{2+x}(s,hyd)) = [PuO_2^+][OH^-]$$

all experimental data in dilute to concentrated electrolyte solutions lead to a consistent value at I = 0, log $K°_{sp}$ = -14.0 ± 0.8 (2σ), which is comparable to the value for $NpO_{2.5}$(s)[3]. The low redox potentials at pH 4 - 13 (regions C in Fig.1) could not be explained[1]. We have shown that they are reproducible (pe + pH = 12.5 ± 1.2), independent of the initial O_2 in the system, and caused by equilibria between PuO_{2+x}(s,hyd), PuO_2^+(aq) and small Pu(IV) colloids/polymers (1.5 - 2 nm) predominant at pH > 7 (log $[Pu(IV)]_{coll}$ = -8.3 ± 1.0).

THERMODYNAMIC DATA

The molar standard Gibbs energy for PuO_{2+x}(s, hyd) = $(PuO_{2.5})_{2x}(PuO_2)_{1-2x}$(s, hyd) can be estimated from the solubility data for x = 0.003 (present study) and x = 0.05 (under air[1]):

$$\Delta_f G°_m(PuO_{2+x}(s,hyd)) = 2x\ \Delta_f G°_m(PuO_{2.5}(s, hyd)) + (1-2x)\ \Delta_f G°_m(PuO_2(s,hyd))$$
$$= \{2x\ (-\ 971.2 \pm 5.4) + (1-2x)(-\ 965.5 \pm 4.0)\}\ kJ/mol$$

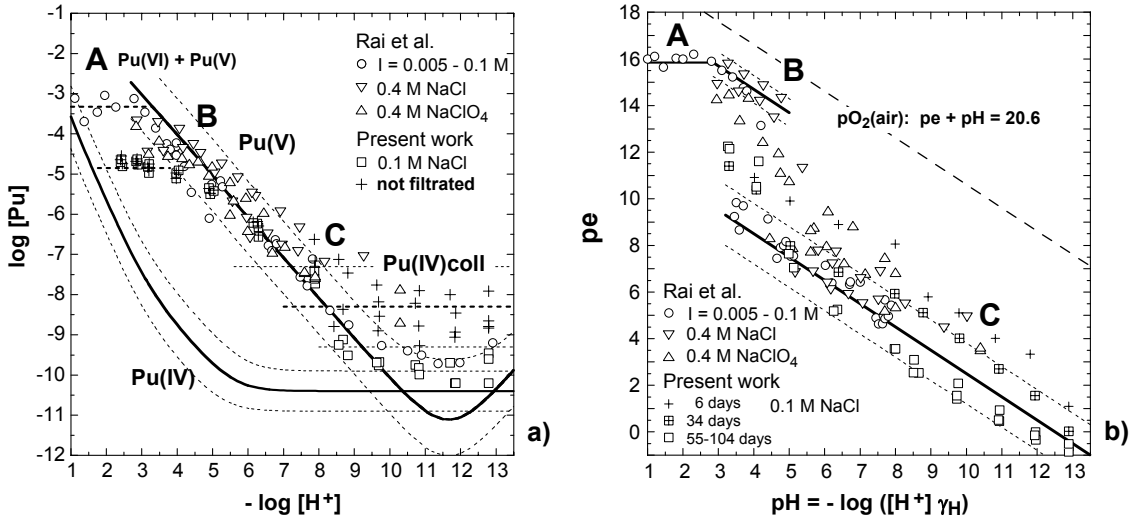

Fig 1: a) Solubility of $PuO_{2+x}(s, hyd)$ at 20 - 25°C; calculated Pu(IV) concentration[4], Pu concentration measured after ultrafiltration (open symbols) and $[Pu]_{tot}$ including Pu(IV) colloids/polymers (crosses), b) simultaneously measured redox potentials (pe = 16.9 Eh(V) at 25°C). Comparison of data from Rai et al.[1] under air and present work under Ar (traces O_2).

Accordingly, $\Delta_f G°_m(PuO_{2+x}(s,hyd))$ is only slightly lower than $\Delta_f G°_m(PuO_2(s,hyd)) = -965.5 \pm 4.0$ kJ/mol[3]. Since the experimental data for $PuO_{2+x}(s,hyd))$ include a certain solid solution stabilization energy, it is not clear whether $PuO_{2+x}(s,hyd))$ can be oxidized to values of $x > 0.27$, the maximum value observed[2]. Possibly, the molar standard Gibbs energy for $PuO_{2.5}(s,hyd)$ is slightly less negative than $\Delta_f G°_m(PuO_2(s,hyd)) = -965.5 \pm 4.0$ kJ/mol. Anhydrous Pu(IV) dioxide ($\Delta_f G°_m(PuO_2(cr)) = -998.1 \pm 1.0$ kJ/mol)[3] cannot be oxidized by $O_2(g)$. Known analogous data and observations for hydrated and crystalline $NpO_2(s)$ and $NpO_{2.5}(s)$ support the calculated thermodynamic data for $PuO_{2+x}(s)$. The values reported by Haschke et al.[2], $\Delta_f G°_m(PuO_{2.25}(s)) = -1080$ kJ/mol and $\Delta_f G°_m(PuO_{2.5}(s)) = -1146$ kJ/mol are much too negative. They are calculated assuming the oxidation of $PuO_2(s)$ by water according to

$$PuO_2(s) + x\ H_2O \rightarrow PuO_{2+x}(s) + x\ H_2(g)$$

For thermodynamic reasons this reaction is not possible ($\Delta_r G°_m > 200$ kJ/mol).

1 D. Rai et al., a) Soil Sci. Am. J. 44, 490 (1980), b) Radiochim. Acta 35, 97 (1984), c) Radiochim. Acta **89**, 491 (2001).

2 J.M. Haschke, T.H. Allen, L.A. Morales, a) Science. 287, 285 (2000), b) J. Alloys Comp. 314, 78 (2001), c) J. Alloys Comp. **336**, 124 (2002).

3 R. Guillaumont et al. (OECD-NEA TDB), Update on the Chemical Thermodynamics of Uranium, Neptunium, Plutonium, Americium and Technetium, Elsevier, 2003.

4 V. Neck, J.I. Kim, Radiochim. Acta, **89**, 1 (2001).

A Look Toward the Future of Solid-State Transuranium Chemistry

T. E. Albrecht-Schmitt*

*Department of Chemistry and Biochemistry and E. C. Leach Nuclear Science Center, Auburn University, Auburn, Alabama 36849

Abstract

In this talk we will investigate recent breakthroughs in solid-state actinide chemistry with a focus on oxide-type materials. We will attempt to look into the crystal ball to see what the future holds in store for this field by looking at recent developments of great importance that will likely have a transforming affect on solid-state actinide chemistry. There have been many exciting disclosures over the past five years that are worthy of highlighting. These topics will including a discussion of nanoscale bonding features in uranyl and neptunyl compounds, magnetic ordering phenomena derived from super-exchange interactions in neptunyl networks, the isolation of a series of Pu(V) compounds that were once thought to be unstable, and unusual bonding in actinide-containing extended networks (Fig. 1). We will look closely at advances in "designing" actinide structures for specific applications, such as ion exchange and nonlinear optics. This will be a far ranging talk intended to peak interest in many aspects of this discipline.

Acknowledgments

This research was sponsored by the U.S. Department of Energy through the Heavy Elements Program.

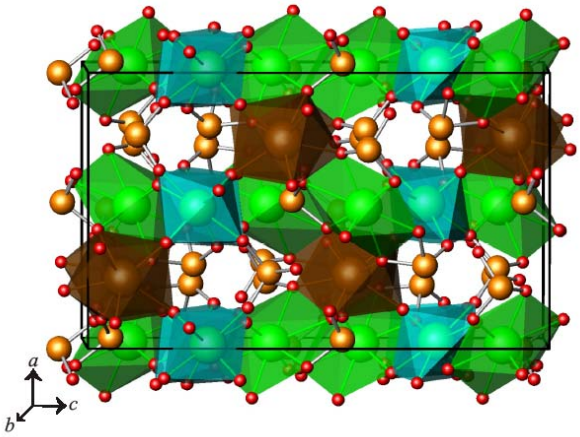

Fig 1: A view of the structure of mixed-valent Np(IV)/Np(V) Selenite, $Np(NpO_2)_2(SeO_3)_3$.

Self-irradiation effects in plutonium alloys

N. Baclet*, B. Oudot*, R. Grynszpan†, L. Jolly*, B. Ravat*, L. Berlu*, G. Jomard#

*Commissariat à l'Energie Atomique, Centre de Valduc, F-21120 Is sur Tille, France
† SERAM, Ecole Nat. Sup. d'Arts et Métiers, F-75013 Paris, France
#Commissariat à l'Energie Atomique, Centre Ile de France, F-91680 Bruyères le Châtel, France

INTRODUCTION

Among the actinides, plutonium is certainly the most complex element due to its intermediate position in the 5f-series, at the edge between localized and itinerant electrons. Most studies focus on plutonium alloys since they can be stabilized at room temperature in the face-centered-cubic phase (δ) by adding deltagen elements such as aluminum, gallium, cerium or americium. The plutonium decay results into the creation of helium and uranium ions, which produce defects through displacement cascades.

EXPERIMENTAL EVIDENCE OF AGING EFFECTS

The self-irradiation defects may affect the plutonium properties and, for instance, induce swelling which amplitude depends on the nature of the solute element and its tendency to segregate in the matrix. Dilatometry and X-ray Diffraction (XRD) have revealed differences in swelling. While XRD shows a microscopic swelling that saturates after about 0.08 displacemens per atoms (dpa) for well homogenized PuGa alloys, macroscopic swelling (as measured by dilatometry) follows a linear trend after a transient period. Swelling might then be the sum of several contributions that affect differently macroscopic and microscopic scales. A better understanding of the basic mechanisms involved in the production of the radiation damages, especially at the early stages, is then required in order to predict their effects on alloyed plutonium. Positron annihilation spectroscopy is an appropriate method to tackle this problem, owing to its specific sensitivity to vacancy-type defects in solids, while lessening radiological constraints by remote measurements. This technique was implemented to monitor the early stages of defect production in as-prepared δ-stabilized PuGa alloys, and to correlate the results with those obtained by dilatometry and XRD. Both types of swelling were investigated versus time. The increase of the positron mean lifetime observed just after casting is associated with an increase in the concentration of vacancy clusters, rather than with an increase in the defects average size, according to the increase in microscopic swelling observed by XRD [1]. Indeed, a size increase of the defects tends to deform the lattice, resulting in the broadening of X-ray lines, whereas an increase in concentration leads to a lattice parameter increase, detected in the present case.

AGING MODELING

However, even if the description of this first stage of defects creation is essential to understand further evolutions, it remains necessary to quantify the changes in physical properties, especially swelling, for much longer periods, for which samples are not available. A multi-scale (time and size) modeling of self-irradiation effects, was therefore developed to

predict the changes. The prime aim was to compare modeling and experiments regarding the swelling data. Moreover, multi-scale modeling might unveil the presence of specific defects required for a more realistic assessment of aging phenomena, and in turn also suggest additional specific experiments for their characterization.

The ab-initio method allows to calculate physical characteristics such as elastic constants, bulk modulus, that are crucial input data to estimate the interatomic potential used for molecular dynamics calculations. Displacement cascades were calculated using the Modified Embedded Atom Model, with a progressive increase in the energy of the uranium recoil atom. Preliminary results for 10 keV reveal that, in the first stage, displacement cascades lead to the formation of an amorphous core of 5 nm average radius containing approximately 5000 Frenkel pairs. At the end of the defects recombination stage (after a couple of nanoseconds), only a few interstitials remain outside the melting zone with an equal number of mono-vacancies within the melting zone [2]. Initial results concerning a 64 keV displacement cascade suggest that sub-cascades appear rapidly. Subsequent diffusion of the defects formed are described with a mesoscopic Monte-Carlo approach, that allows to calculate swelling induced by the remaining defects, and to compare directly to experimental data. In parallel, a more phenomenological approach, based on rate equations has been developed and compared to the Monte Carlo approaches.

Whatever the scale, modeling must be validated through comparison with experimental data. Dedicated experiments have therefore been designed to measure the plutonium physical properties required by the theoretical approach. For example, molecular dynamics simulation of displacement cascades depends strongly on the choice of the interatomic potential. This complex potential is adjusted using experimental data such as elastic constants. Consequently, we designed X-ray diffraction (XRD) experiments to extract single crystal elastic constants from measurements performed on a polycrystal of δ-Pu alloy. Moreover, the number of defects induced by a α-decay is directly determined by the displacement threshold energy E_d, not hitherto measured for plutonium. Hence, a low-temperature electrical resistivity setup was designed to measure E_d in electron-irradiated plutonium. Furthermore, isochronal annealing should also allow the measure the migration energy of the various defects. All these experimental results should contribute to the validation of both ab-initio and molecular dynamics calculations and will be used as input data in Monte-Carlo methods.
Recent results regarding the different physical properties cited above will be presented.

1 B. Oudot, PhD Thesis, Université de Franche-Comté, Besançon, France (2005).
2 L. Berlu, G. Rosa, P. Faure, N. Baclet and G. Jomard, MRS Fall Meeting, Boston, (2005).

First principles determination of the vacancy formation energy in δ-plutonium

G Robert*, A. Pasturel†, B. Siberchicot*

*CEA-DIF BP 12, F-91680 Bruyères-le-Châtel, France

†Laboratoire de Physique et Modélisation des Milieux Condensés, CNRS
25 avenue des Martyrs, BP 106, F-39042 Grenoble, France

Abstract :

One of the most tricky problems concerning the δ fcc-stabilized phase of plutonium consists in predicting its properties under long-term aging.
Due to its radioactive nature, the unstable plutonium nucleus decays principally by α- decay. Two types of defects, namely vacancies and self-interstitials, are formed in metals by this self irradiation.
The evolution of defect population can lead to significant changes in the microstructure and causes a number of radiation-induced macroscopic properties changes such as density, ductility or elastic constants.
Due to the special location of plutonium at the boundary between light actinides (delocalized 5f electrons) and heavy actinides (localized 5f electrons) a slight change in atomic volume or internal stresses could affect its stability.
Concerning the knowledge of the thermodynamic and kinetic behavior of metals, one of the most important quantity is the vacancy formation energy. Its determines the equilibrium vacancy concentration and contributes to the self-diffusion coefficient in the monovacancy mechanism, which is the main diffusion process in the closed-packed metals. Then the activation energy is the sum of the vacancy formation energy and of the migration energy of the vacancy. Due to the lack of experimental values concerning defects in plutonium [1] and its alloys, first-principles calculations are of considerable interest to estimate the formation energies of point defects in these phases.
In this aim, we study the stability and formation energies of vacancies in plutonium with spin-polarized PAW calculations using the Vienna ab initio simulation package VASP [2][3].

Even if magnetism in δ-Pu has not been confirmed by experiment [4][5], taking into account magnetic exchange interaction leads to major improvements compared to standard non-magnetic LDA or GGA results.

As already shown in these previous papers [6][7][8][9] spin polarized GGA approximation is able to reproduce the main equilibrium properties and energy differences of pure and alloyed plutonium.

In these presentation, we follow these ideas and expand the investigation to study the influence of magnetic configuration on the vacancies energies in δ-plutonium. The calculations were performed for three different configurations, namely : antiferromagnetic (AF), ferromagnetic (FM) and disordered magnetic structures (DM). We also evaluate box-size effects and local relaxations with these three magnetic configurations. Some results have already been reported in an earlier paper [10].

The first interesting result is that the unrelaxed values of both mono and divacancies are not very sensitive to the long range magnetic ordering.
The other important point is that the formation of divacancies do not require an additional energy with respect to the formation of two isolated monovacancies. This indicated that vacancy clusters are as stable as isolated vacancies.
Now, if we allow atomic relaxation, the inward relaxation is of order of 3 % (7 % for divacancies), as usually obtained for transition metals.
The energy of the divacancy is still similar to the energy of two isolated vacancies. Nevertheless, the relaxed energy and forces acting on atoms is function of magnetic configuration.

1 M.J. Fluss, B.D. Wirth, M. Wall, T.E. Felter, M.J. Caturla, A. Kubota, T. Diaz de la Rubia, J. Alloys. Comp. **368**,62, 2004
2 G. Kresse and J. Furthmüller, Phys Rev B **54**,11169 (1996)
3 G. Kresse and J. Furthmüller, Comput. Mater. Sci. **6**,15 (1996)
4 N.J. Curro and L. Morales, Mat. Res. Soc. Symp. Proc. **802**, 53 (2004)
5 R.H. Heffner, G.D. Morris, M.J. Fluss, B.Chung, D.E. MacLaughlin, L. Shu and J.E. Anderson, in press, Physica B
6 Y. Wang and Y.F. Sun, J. Phys. Condens. Mater. **21**,L311 (2000)
7 P. Soderlind, A. Landa, B. Sadigh, Phys. Rev. B 66,205109 (2002)
8 G. Robert, C. Colinet, B. Siberchicot and A. Pasturel, Modelling Simul Mater Sci. Eng **12**,693 (2004)
9 B. Sadigh, W.G. Wolfer, Phys. Rev B **72**,205122 (2005)
10 G.Robert, A. Pasturel, B. Siberchicot, Europhysics Letters 71,3,412 (2005)

Monte Carlo + Molecular Dynamics simulation of radiation damage evolution in Pu

V.V. Dremov, P.A. Sapozhnikov, S.I. Samarin, D.G. Modestov, N.E. Chizhkova

Russian Federal Nuclear Centre – Zababakhin Institute of Applied Physics (RFNC-VNIITF)
Snezhinsk, Russia 456770

ABSTRACT

The paper presents results obtained in the simulation of damage cascades in self-irradiated unalloyed and gallium-alloyed delta-plutonium. The fast cascade stage was simulated by Monte Carlo method. It follows from Monte Carlo calculations that in a cascade formed by a uranium nucleus of energy 86 keV, about 40% of the initial energy is lost in inelastic collisions with electrons and the rest energy resides in the crystal lattice. When the energies of cascade particles became close to the displacement energy, the cascade configuration resulted (coordinates + particle velocities) was transferred to a molecular dynamics (MD) code which helped track the further evolution of the system to ~1-2 ns. The Modified Embedded Atom Model (MEAM) [1,2] was used to describe particle interactions.

Our simulations show that a cascade from the uranium recoil nucleus causes a large energy release into a lattice subsystem within a local region measuring about 20-25 nm; this causes material melting and subsequent recrystallization. Preliminary estimates showed that the energy transferred to the lattice is enough to cause melting in a region which characteristic size reaches 15 nm; the region contains ~200 000 atoms. MD simulations show that lattice heat conductivity reduces the characteristic size of the melting region to ~8-10 nm (~35 000 atoms) in a sample whose initial temperature was 300K.

The evolution of temperature and density fields in the damaged region was tracked in simulations. The time of recrystallization was estimated to be ~1ns. The distribution of point defects in the recrystallized region was obtained. Most of point defects created during a fast stage of the cascade vanish when melting and recrystallizing, residual defects evolve much slower than the nano-second time scale

The calculations have also been carried out for polycrystalline samples. If the damaged region is inside a single-crystal grain, the melted material undergoes complete recrystallization when cooling. If radiation melting occurs in a region which contains a grain boundary, the recrystallization in the melted regions adjacent to different grains will differ. Such a process results in grain boundary sagging and broadening with time. As an illustration Figure 1 shows the same fragment of a sample containing a grain boundary at the moment of maximum size of melted region (left picture, t=20 ps) and at the moment 1 ns (right picture) when the process of recrystallization is almost completed.

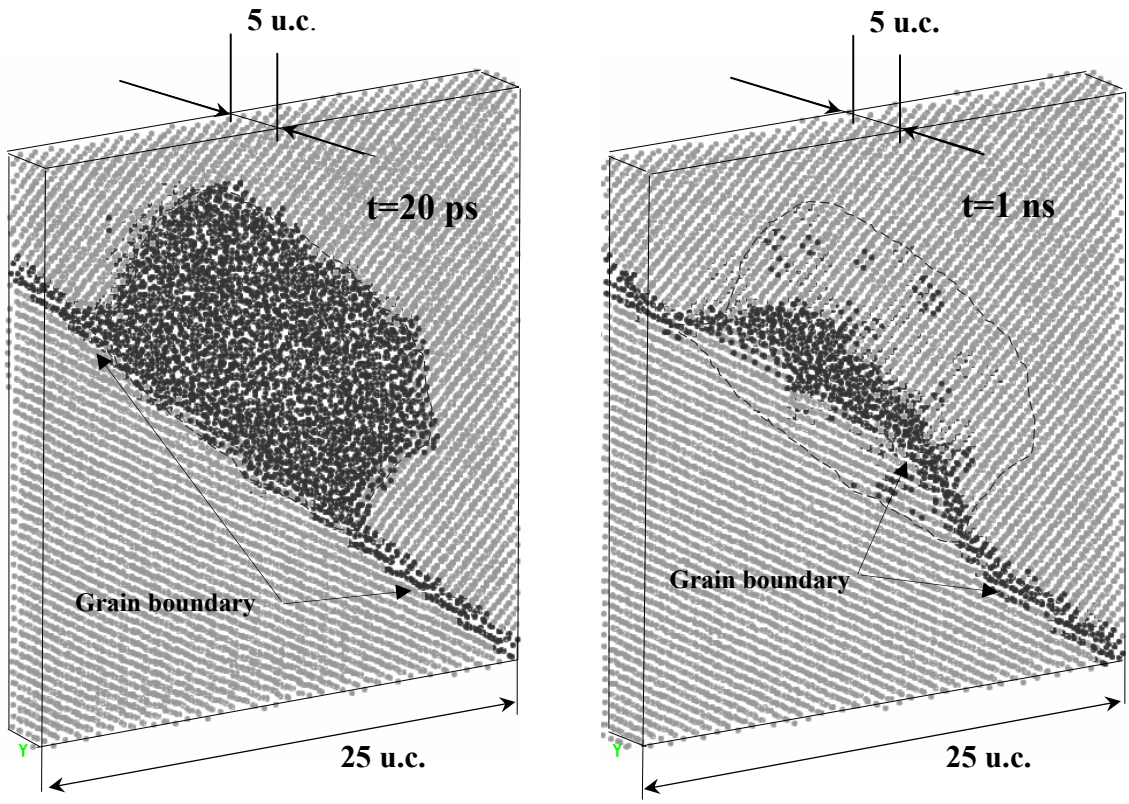

Fig.1 Fragments of a polycrystalline sample containing grain boundary adjacent to the damaged (melted) region. Taupe color is for disordered structure (grain boundary, melted region), light grey color if for fcc δ-Pu. Dashed line contours the region where the recrystallization took place.

1. M. I. Baskes, *Phys. Rev. B*, v. 62 (2000), p. 15532.
2. M. I. Baskes, K. Muralidharan, M. Stan, S. M. Valone, F. J. Cherne, *JOM* 55 (2003), p. 41.

Collective Effects in PuGa Alloys and Their Effects on Structure, Phase Stability, and Radiation Damage Mechanisms

Steven D. Conradson
Los Alamos National Laboratory, Los Alamos NM 87544 USA

Local structure measurements, particularly the element specific information afforded by EXAFS studies at the Pu, Ga, In, Ce, and U edges, show evidence for collective behavior among these minority elements that are present at only a few atom percent and are never observed to be directly bonded in significant amounts. Certain aspects of the concentration dependence of the EXAFS are consistent with the Ga atoms being "organized" within the delta host to give a semi-ordered, quasi-intermetallic phase with a Pu:Ga ratio of around 30:1. In this the Ga atoms would have higher probabilities of being at certain distances and angles with respect to each other without being at positions specific enough to modify the diffraction pattern from that of a random solid solution with a cubic structure. However, this long-range clustering is sufficient to promote the formation of nanoscale regions that are locally depleted in Ga below the saturation limit at around 3.3 at-% Ga. If separated from the host delta lattice the up to 20% of the Pu atoms within these volumes would form alpha Pu. However, because of the tensile stress (negative pressure) and epitaxial constraints exerted by the host, it instead forms a second, ordered, novel structure called "sigma" (Fig. 1). Sigma Pu consists of a modulated, expanded Fm3m arrangement of atoms that must also contain some interstitials to retain the delta density. In addition, In- and Ce-based delta Pu alloys show analogous kinds of behavior that imply that, even when the elastic strain is minimal because the alloys atoms are close in size to Pu, there are still strong interactions between relatively distant minority atom sites that disrupt the arrangement of Pu atoms around them and also cause long range organization and clustering.

This heterogeneity and corollary nanophase separation is critical in aging, most likely accounting account for the very large (tens of percent) numbers of Pu atoms displaced from the delta lattice in aged materials. As with the sigma structure, these atoms appear to form additional types of ordered structures so that the radiation damage does not result in the Pu becoming "glassy" through decades of normal aging (Fig. 1). The radiation effects do ultimately affect phase stability however, so that causing the reversible martensitic transformation through the alpha phase that does not foster radiation damage produces some very unusual effects. These results are perhaps best explained and reconciled with other macroscopic properties in terms of describing the material with a dynamic energy landscape incorporating rehybridization induced by local composition and strain that results in multiple stable shapes for the Pu atoms and multiple structures for the nanophases.

Figure 1. Pu $\chi(R, k^2)$ residuals obtained by subtracting the curve-fit with only the δ shells of atoms from the spectra from k=3.7–14.8 $Å^{-1}$. Over this range a simple Pu shell will give a spectral feature in which the real component gives a minimum close to where the modulus peak is located and somewhat symmetric maxima on each side, features with a different pattern indicate more complex types of structures. The lines act as approximate guides to features

exhibited by several spectra that are associated with the σ and σ' structures, the δ structure, initial radiation damage in 1.7 at-% Ga materials (d-i) and longer duration damage in materials with higher [Ga] and AAP (d). Features below 2.5–3.0 Å that are not common to several samples are most likely low frequency residuals from incomplete background subtraction due to, e.g., a small Am edge in the spectrum or other low frequency artifacts. A spectrum of α Pu reduced in amplitude by a factor of 5 is included with the standards for comparison with the σ' feature.

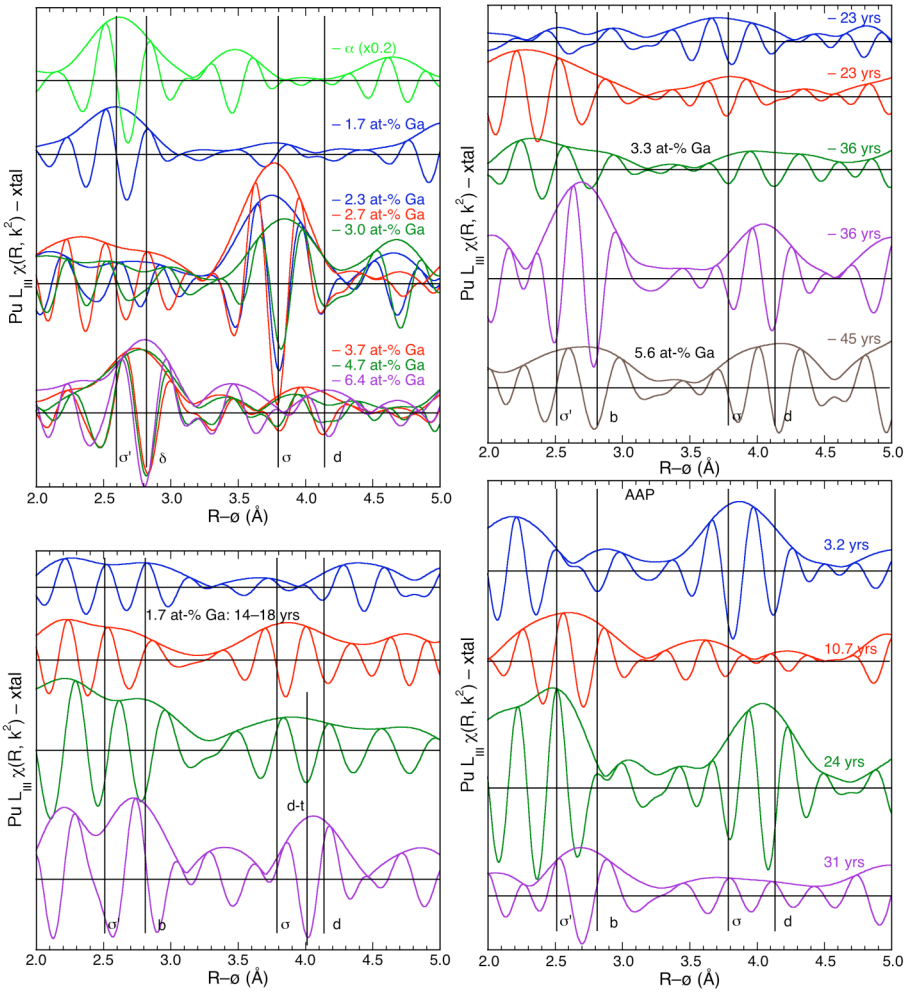

Acknowledgements. *This work was supported by the Heavy Element Chemistry Program, Chemical Sciences, Biosciences, and Geosciences Division, Office of Basic Energy Sciences, and the Enhanced Surveillance Campaign, National Nuclear Security Adminstration, U.S. Department of Energy under contract W-7405. XAFS and XRD were performed at SSRL (Stanford Linear Accelerator Center) and APS (Argonne National Laboratory), which are operated by the US Department of Energy, Office of Basic Energy Sciences. Health Physics operations at SSRL and APS were supported by the Seaborg Institute for Transactinium Science at LANL.*

The Actinides – a beautiful ending of the Periodic Table

B. Johansson[*,†]

[*]Condensed Matter Theory Group, Department of Physics, Uppsala University, BOX 530, SE-751 21, Uppsala, Sweden
[†]Applied Materials Physics, Department of Materials Science and Engineering, Royal Institute of Technology, SE-100 44 Stockholm, Sweden

The series of heavy radioactive elements known as the actinides all have related elemental properties. However, when the volume per atom in the condensed phase is illustrated as a function of atomic number, perhaps the most dramatic anomaly in the periodic table becomes apparent. The atomic volume of americium is almost 50% larger than it is for the preceding element plutonium. For the element after americium, curium, the atomic volume is very close to that of americium. The same holds also for the next elements berkelium and californium. Accordingly from americium and onwards the actinides behave very similar to the corresponding rare-earth elements – a second lanthanide series of metallic elements can be identified. This view is strongly supported by the fact that all these elements adopt the dhcp structure, a structure typical for the lanthanides.

The reason for this behavior is found in the behavior of the 5f electrons. For the earlier actinides, up to and including plutonium, the 5f electrons form metallic states and contribute most significantly to the bonding. In Np and Pu they even dominate the bonding, while all of a sudden they become localized in Am, very much like the 4f electrons in the lanthanide series, and contribute no longer to the cohesion. This withdrawal of 5f bonding gives rise to the large volume expansion between plutonium and americium. This difference between the light and heavy actinide suggests that it would be most worthwhile to strongly compress the transplutonium elements, thereby forcing the individual 5f electron wave functions into strong contact with each other (overlap). Recently high pressure experiments have been performed for americium and curium and dramatic crystal structure changes have been observed. These results and other high pressure data will be discussed in relation to the basic electronic structure of these elements. We will also discuss some other recent high pressure data for the earlier actinides. Here it becomes important to establish to what extent standard density functional theory can account for the observed behavior.